Improving the thermal properties of fluoroelastomer (Viton GF-600S) using carbon nanotube

Javad Heidarian, Aziz Hassan & R. A. Lafia-Araga

Published online: 05 Jan 2016.

Submit your article to this journal ⌐

View related articles ⌐

View Crossmark data ⌐

Taylor & Francis
Taylor & Francis Group

Improving the thermal properties of fluoroelastomer (Viton GF-600S) using carbon nanotube

Javad Heidarian[a,b], Aziz Hassan[a] and R. A. Lafia-Araga[a]

[a]Department of Chemistry, Polymer and Composite Materials Research Laboratory, University of Malaya, Kuala Lumpur, Malaysia; [b]Nanotechnology Research Centre, Research Institute of Petroleum Industry-RIPI, Tehran, Iran

ABSTRACT

Nanocomposites were prepared using carbon nanotubes (CNTs) in the formulations of fluoroelastomer (FE). Thermogravimetric analysis (TGA) results revealed that CNT improved the thermal properties of FE, resulting in higher amount of FE and char remaining within the temperature range of 520–900 °C, relative to unfilled FE and carbon black (CB)-filled FE. The same results also revealed that more percentage of FE was undegraded or less degraded especially near CNT. Energy dispersive X-ray (EDX) results indicated that the percentage of carbon and fluorine in the residue of TGA scans up to 560 °C of CNT-filled FE (CNT/FE) were higher compared to the CB-filled FE (CB/FE), and CB/FE was higher than FE. EDX results of TGA residue (run up to 900 °C) showed that most of the undegraded FE which was not degraded at temperatures below 560 °C was degraded from 560 °C to 900 °C in both CNT/FE and CB/FE, with the char in CNT/FE being more than that in CB/FE. Residue of samples after TGA scans up to 900 °C indicated that, Zn did not undergo any reaction with CNT in the CNT/FE. In CB/FE, some percentage of ZnO reacted with carbon. EDX analysis of thermal aged specimens under air showed that with increasing aging time, more percentage of C, O, and F were lost from the surface of filler/FE and FE. The order of element loss is: CNT/FE < FE < CB/FE.

1. Introduction

Viton is a synthetic rubber and a fluoroelastomer (FE) which is used in manufacturing O-rings and other molded and extruded articles manufactured by E. I. du Pont de Nemours and Co., USA.[1] Viton® GF-600S is the latest development in Viton GF family, a terpolymer of hexafluoropropylene, vinylidene fluoride, and tetrafluoroethylene with a cure site monomer. Formerly known as VTR-8600, it is a next generation, easy processing, and peroxide cure, 70% fluorine FE based on new Advanced Polymer Architecture (APA). Compared to the original GF family, Viton® GF-600S exhibits better processability, coupled with similar or improved fluids resistance.[1, 2]

CONTACT Javad Heidarian ✉ heidarianj@um.edu.my

CNT improves the properties of fluoropolymers, such as crystallinity, electrical response, mechanical properties, viscoelastic behavior, etc., and therefore their thermal stability. This finding has been reported by a number of researchers and examples of literatures and the reasons for the changes in these properties are mentioned bellow. CNT is also expected to improve thermo-oxidative degradation resistance of FE composites when subjected to thermal aging conditioning in air.

Rubber sealants or O-rings are major components in enabling the probing and production of oil in deeper wells, so that higher temperature and pressure reservoirs are reached. In this account, it is demonstrated that carbon nanotube (CNT) homogeneously and randomly dispersed in rubber matrices, are able to generate durable sealants that operate satisfactorily at high temperatures and pressures. It has been reported [3] that, the use of multi-walled carbon nanotubes (MWCNTs) embedded in fluorinated rubber leads to a rubber nanocomposite with cellulation structure, possessing improved performance, leading to a balanced pressure resistance, sealing ability, thermal resistance, and durability. The O-rings made by this rubber nanocomposite have high sealing properties and are durable up to 260 °C and 239 MPa. They exhibit better pressure resistant properties relative to carbon black (CB)-filled composites by about 80–100 MPa higher, which corresponds to a much deeper depth in water of 8000 m. In addition, they show higher resistance than the fluorocarbon elastomer material (FKM)-derived O-ring in both low- and high-temperature ranges. FKM is the designation of about 80% of fluoroelastomers as defined by ASTM D-1418. All FKM fluoroelastomers contained vinylidene fluoride.

Strong interaction between fluoropolymers and CNT was reported by He et al. [4]. The authors observed that in dynamic mechanical measurements, storage modulus is significantly increased due to this interaction. High aspect ratio of nanotubes also leads to a great increase in the active interfacial area between CNT and fluoropolymer chain as reported by Chae et al. [5].

The preparation and characterization of FE/MWCNTs nanocomposites by conventional rubber mixing using a two-roll mill has been reported by Pham et al. [6]. The authors observed that with increasing MWCNT loading, there was a steady increase in decomposition temperature.

There is a growing requirement for seals in the automotive fuel system connections to have electrostatic dissipation properties. Fluorocarbon (FKM) elastomeric O-ring seals are a significant component in the conductive pathway. Russell et al. [7] reported that providing this conductivity through the incorporation of CNTs considerably improves properties over the use of carbon blacks (CBs). This results in a seal which is softer with improved processability, stable electrical properties, and better permeation resistance.

Energetic relationship between surface of CNT and fluoropolymer was reported by Levi et al. [8]. It was reported that fractured surface of composite leaves the CNT with a polymer coating. The coating can be quite thick and covers the length of CNT. Thus, during pullout, this polymer sheet remains associated with CNT.

Normally, in the formulation of Viton, CB is used. Replacing CB with CNT partially or totally is expected to improve the thermal, physical, mechanical, chemical, and other properties of the Viton which are very effective in making O-rings especially for oil and gas industries.[3, 6, 9]

Some changes in the properties of fluoropolymers due to the presence of CNT were reported by a number of researchers. CNT can change mechanical and thermo-mechanical

properties of polyvinilydienefluoride (PVDF) [10–12] or mechanical properties of polytetrafluoroethylene (PTFE).[13,14] CNT can also change the degree of crystallinity of fluoropolymers and therefore, the properties.[15–17] Fluoropolymers/CNT interfacial interaction also had a profound influence on melt rheological behavior of these nanocomposites.[18] Thermal stability of the PTFE composites is also enhanced by the presence of CNT.[19]

X-ray photoelectron spectroscopy (XPS), scanning electron microscopy and electron probe X-ray microanalysis (SEM/EPMA), and X-ray diffraction (XRD) analysis were used to elucidate the physical and chemical changes associated with degradation on the surface, near surface, and bulk of the FE seals in engine oil and additives.[20] Degradation of these materials was reported to be limited to the near surface region of the samples to the depth of less than approximately 50 μm. The process results in release of either F_2 or HF.

Research on the verification of the effect of CNT on the amount of residues in TGA runs of CNT/FE nanocomposites is rather rare. In addition, the comparison of the amount of residue of the TGA runs of FE, CB/FE, and CNT/FE, detailing the elemental compositions is seldom published. Therefore, this investigation is unique in the sense that knowledge of the amount of residue and the composition of the elements in the residue give an insight into the ability of CNT to improve the thermal stability of CB/FE and FE composites. Furthermore, the presence of elemental fluorine on the surface of CNT/FE, CB/FE, and FE aged in air indicates that CNT improves the resistance of the nanocomposites to thermo-oxidative degradation.

In the present work, CNT was used as filler for Viton® GF-600S with the aim of improving thermal stability and thermal aging resistance of FE. The thermal properties of the composites vis-à-vis CB filled and unfilled FE were assessed by thermogravimetric analysis (TGA). Energy dispersive X-ray (EDX) was also used to characterize the elemental composition of the undegraded FE and char after TGA runs at temperatures below 900 °C. This is to ascertain whether incorporation of CNT can preserve more of the undegraded FE and char compared to CB-filled FE or unfilled FE in TGA runs. EDX was also employed to verify the amount of Zn in the residue and to confirm possible reaction with CNT or CB. Thermal aging conditioning in air together with EDX was also conducted to investigate the elemental composition of the surfaces of unfilled and filled FE as a function of aging time.

2. Experimental

2.1. Materials and compounding procedure

Materials used were Viton GF-600S fluoroelastomer, FE; organic peroxide, Luperox 101 XL-45; carbon nanotube, CNT (TNM8, outside diameter > 50 nm, purity > 95%, and length of 10–20 μm); carbon black, CB Ensaco 250; zinc oxide; and triallylisocyanurate, TAIC supplied by ERIKS Sdn. Bhd. (Malaysia), Arkema Sdn. Bhd. (Malaysia), Chengdu Organic Chemicals Co. Ltd. (Chinese Academy of Sciences, China), Age D'Or Industrial Sdn. Bhd. (Malaysia), Texchem Materials Sdn. Bhd. (Malaysia) and Liu Yang San Ji Chemical Trade Co. Ltd. (China), respectively. Three formulations were compounded, CNT-filled FE (CNT/FE), CB-filled FE (CB/FE) and unfilled FE (FE). In all compounds, the amount of FE, organic peroxide, zinc oxide, and TAIC were 70.0, 2.1, 2.1, and 2.1 g, respectively. For CNT/FE and CB/FE, 7.0 g filler was used.

Mixing FE with additives was done using a laboratory scale two-roll mill with a roll temperature of 48 °C. FE in the above-mentioned composition was supplied to open roll. A uniform band was formed while three rolling cuts from each side of the mill were made, so that the polymer turned into uniform and sufficiently warmed up. In the next stage, pre-blended ZnO and TAIC were added uniformly into the gum and three rolling cuts from each side of the mill were done. After setting the roll distance to 1.1 mm, CNT was then fed in. The compound was then tight milled 10 times. The roll distance was then adjusted to 1.1 mm, and the peroxide was added and after final five to six rolled up end passes, the mixture was supplied to the open roll and sheeted. After 24 h, re-milling was done with a roll temperature of 26 °C. Similar procedure was used for CB/FE and FE.

2.2. Curing and post curing

Curing of FE compound was done with the mold (15 cm × 15 cm × 1 mm) in a heated press, at 177 °C under pressure of 10 MPa for 7 min. The post-curing was done in air oven at 232 °C for 2 h. Conditions for curing and post-curing were recommended by the supplier.

2.3. Characterization

2.3.1. Thermal gravimetric analysis

TGA runs from room temperature to 900 °C were carried out on a Perkin-Elmer Pyris Diamond TG/DTA thermal analysis system at a scan rate of 20 °C min^{-1} under nitrogen atmosphere of 20 ml min^{-1}. In addition, TGA runs from room temperature to 560 °C were carried out under the same condition and then cooled to room temperature at a scan rate of 100 °C min^{-1}. The same procedure was repeated with the temperature raised to 900 °C. The specimens were designated as, for example CNT/FE-560 °C, where the temperature after the specimen designation is the highest temperature of the TGA run.

2.3.2. Thermal aging

Thermal aging was done according to ASTM D-573 for 24, 48, and 72 h at 250 °C in air oven. The samples (5 mm × 5 mm × 2 mm) were named FE, FE-24, FE-48, and FE-72, where the numbers following FE indicate the aging time in hour. Similar styles of abbreviations were used for CB/FE and CNT/FE aged samples.

2.3.3. Energy dispersive X-ray and field emission scanning electron microscopy (FESEM) image analyses

EDX analysis was conducted using FESEM Philip XL-40 (UK) coupled with EDX. The residue obtained from heating–cooling TGA scans was first applied on aluminum stub using double-sided copper tape (3 M Company), coated with gold for an EDX elemental analysis to determine the elements of C, O, F, Si, Ca, and Zn.

Elemental compositions of the surfaces of the aged and unaged samples were obtained using EDX. The major elements characterized were C, O, F, and Si. The surface images for some of the samples were obtained by FESEM. In FESEM imaging of CNT/FE, the razor cut (cross section) surface was used. For other specimens, the normal flat surface was used. Specimens for EDX and FESEM imaging analysis were applied on a copper tape and gold coated as mentioned above.
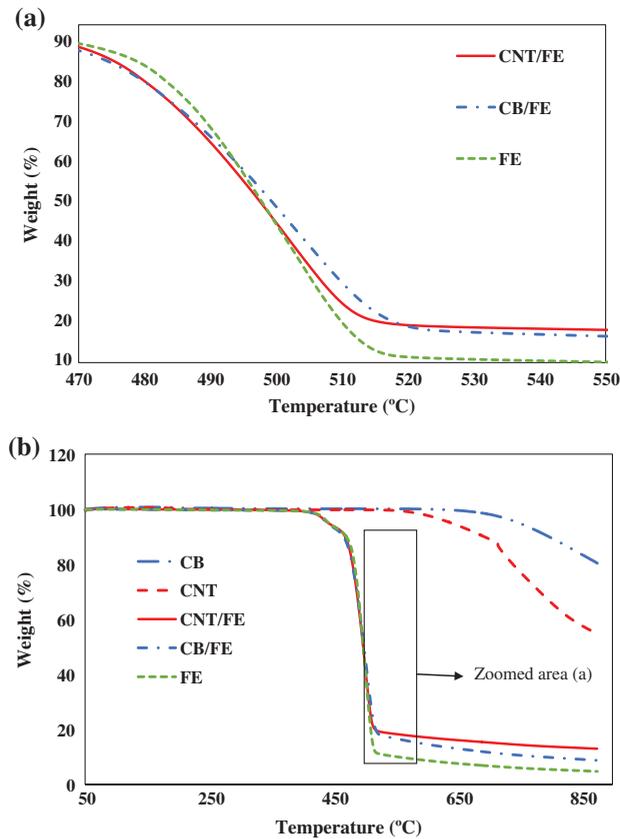
Figure 1. TGA curves of pure filler, FE and filler/FE; (a) zoomed and (b) unzoomed.

Table 1. TGA thermal properties of FE, filler/FE, and pure filler.

Specimen	T_{Onset} (°C)	$T_{5\%}$ (°C)	$T_{10\%}$ (°C)	$T_{50\%}$ (°C)
CB	720.0	748.8	797.6	–
CNT	589.6	639.3	693.1	–
FE	423.4	442.6	470.7	497.8
CB/FE	420.7	439.6	465.8	499.9
CNT/FE	418.9	441.2	468.5	497.7

3. Results and discussion

3.1. Thermal gravimetric analysis

Figure 1 shows the TGA thermograms of CB, CNT, FE, CB/FE, and CNT/FE. The extracted data from these plots are presented in Table 1. In Table 1, T_{onset}, $T_{5\%}$, $T_{10\%}$, and $T_{50\%}$ are the onset temperatures at which the compound starts to lose weight (degrade), temperature at which the compound loses 5, 10, and 50% weight, respectively. T_{onset}, $T_{5\%}$, $T_{10\%}$, and $T_{50\%}$ are almost the same for CNT/FE, CB/FE, and FE. It shows that CNT does not really affect these parameters of CNT/FE compared to CB/FE or FE. However, incorporating of CNT affects the TGA-weight of residual of CNT/FE in the temperatures range of 520–900 °C compared to others.

Table 2. The percentage of filler remaining in pure filler and filler/FE at different temperatures.

Temperature (°C)	CNT (%)	CNT/ FE (%)	CB (%)	CB/FE (%)
523	100.0	8.4	100.0	8.4
542	99.7	8.4	100.0	8.4
562	99.3	8.3	100.0	8.4
600	97.9	8.2	100.0	8.4
650	94.5	7.3	99.7	8.3
700	89.3	7.5	98.3	8.3
800	66.6	5.6	90.0	7.6
875	54.8	4.6	80.4	6.8

Table 3. The percentage of 'undegraded FE + char + mineral additives' and 'undegraded FE + Char' remained in the compounds at different temperatures.

Temperature (°C)	'undegraded FE + char + mineral additives'			'Undegraded FE + Char'
	FE	CB/FE	CNT/FE	CNT/FE
523	10.4	9.9	10.8	8.3
542	9.4	8.9	10.1	7.6
562	9.2	7.6	9.6	7.1
600	7.9	6.6	8.8	6.3
650	7.0	5.1	8.7	6.2
700	6.1	3.6	7.6	5.1
800	4.9	2.4	7.6	5.1
875	4.3	1.9	7.6	5.1

3.1.1. TGA – weight of residual

Figure 1 shows that with incorporating of CNT, a higher amount of the FE residue remained in the temperature range of 520–900 °C compared to CB/FE or FE. Besides, in CNT/FE, most of the char is stable up to 900 °C while in CB/FE, most of the char decomposed, degraded, and evaporated.

Pham et al. [6] used SEM micrograph of the ash residue collected after 90% degradation of the compound and showed that less or partial degradation of the polymer chains attached to the nanotubes occur, whereas extensive degradation occurred in the bulk. Based on amount of FE remaining in the temperature range of 520–900 °C and the previous reported work,[6] it can be seen that the FE attached to or near the CNT within this temperature range will not be degraded or degrade less, and more percentage of FE and char was preserved compared to CB/FE or FE. Therefore, the presence of CNT enhances thermal stability of FE, resulting in higher percentage of the nanocomposite remaining undegraded at higher temperatures.

The percentage of 'CNT remaining' within the nanocomposite can be calculated by multiplying the percentage of CNT obtained from the TGA data of pure CNT at that temperature by 8.4 (the initial percentage of CNT in FE). These amounts are shown in Table 2. From Figure 1 and Table 2, it can be seen that pure CNT lost more weight at temperatures up to 900 °C than pure CB. Again, in the TGA of the nanocomposite, at each temperature, the percentage of 'undegraded FE + char + mineral additives' can be calculated by subtracting the percentage of 'CNT remaining' in the nanocomposite (Table 2) from the percentage of nanocomposite remained in TGA curve extrapolated in Figure 1 at that temperature. Results of these calculations are shown in Table 3. This amount, minus the initial mineral filler will give the percentage 'undegraded FE + char' as tabulated in the same table. For example, from TGA run of pure CNT in Figure 1 (b) at 650 °C, the weight loss percentage
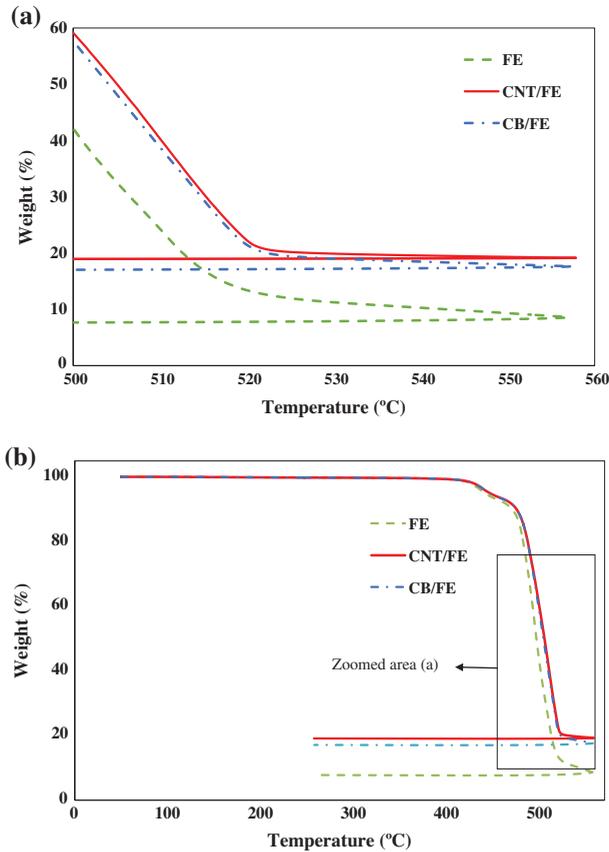
Figure 2. Heat and cool TGA curves of FE and filler/FE up to 560 °C; (a) zoomed and (b) unzoomed.

is 5.5 and the remained CNT percentage is 94.5. This means in the TGA run of CNT/FE at 650 °C in the same figure, the CNT part of nanocomposite lost 5.5% of its initial weight, and 94.5% of CNT initial weight was remained. Because in nanocomposite the initial weigh percentage of CNT is 8.4, therefore the CNT remained in nanocomposite is equal to multiplication of 0.945 (94.5% in decimal form is equal to 0.945) and 8.4 which is equal to 7.3%. In TGA graph of CNT/FE, 15.8% of initial weight of CNT/FE at 650 °C remained. Therefore, the subtraction of 15.8 and 7.3 (CNT/FE and CNT weight percentage remained at this temperature respectively) which is equal to 8.5 is the weight percentage of 'undegraded FE + char + mineral additives' at this temperature in CNT/FE. For the other temperatures, these amounts are shown in Tables 2 and 3. The same calculations were done for CB/FE.

3.1.2. EDX analysis – residual elemental

The compositions of the residue from heating–cooling TGA run cycle, as mentioned in experimental section, were characterized by EDX. TGA curves of the samples are shown in Figure 2. In the heating–cooling run, the cooling was done with the highest possible cooling rate in order to prevent further degradation and keeping the same composition of the remaining materials at 560 °C and at 900 °C upon cooling. Table 4 shows the elemental

Table 4. The weight% (wt%) and atomic% (at%) composition of the remaining composites in TGA runs.

Element	FE-560 °C		CB/FE-560 °C		CNT/FE-560 °C		CB/FE-900 °C		CNT/FE-900 °C	
	Wt%	At%	Wt%	At%	Wt%	Wt%	At%	Wt%	At%	Wt%
C	27.2	50.5	63.6	77.4	68.9	80.8	76.5	89.5	65.4	83.6
O	14.0	19.5	13.7	12.5	10.1	8.9	6.2	5.4	9.0	8.6
F	11.1	13.0	8.9	6.8	10.5	7.8	2.5	1.8	2.5	2.1
Si	–	–	–	–	0.5	0.2	–	–	–	–
Ca	3.0	1.7	1.7	0.6	0.8	0.3	1.2	0.4	2.1	0.8
Zn	44.7	15.3	12.1	2.7	9.2	2.0	13.7	2.9	21.0	4.9
Total	100	100	100	100	100	100	100	100	100	100
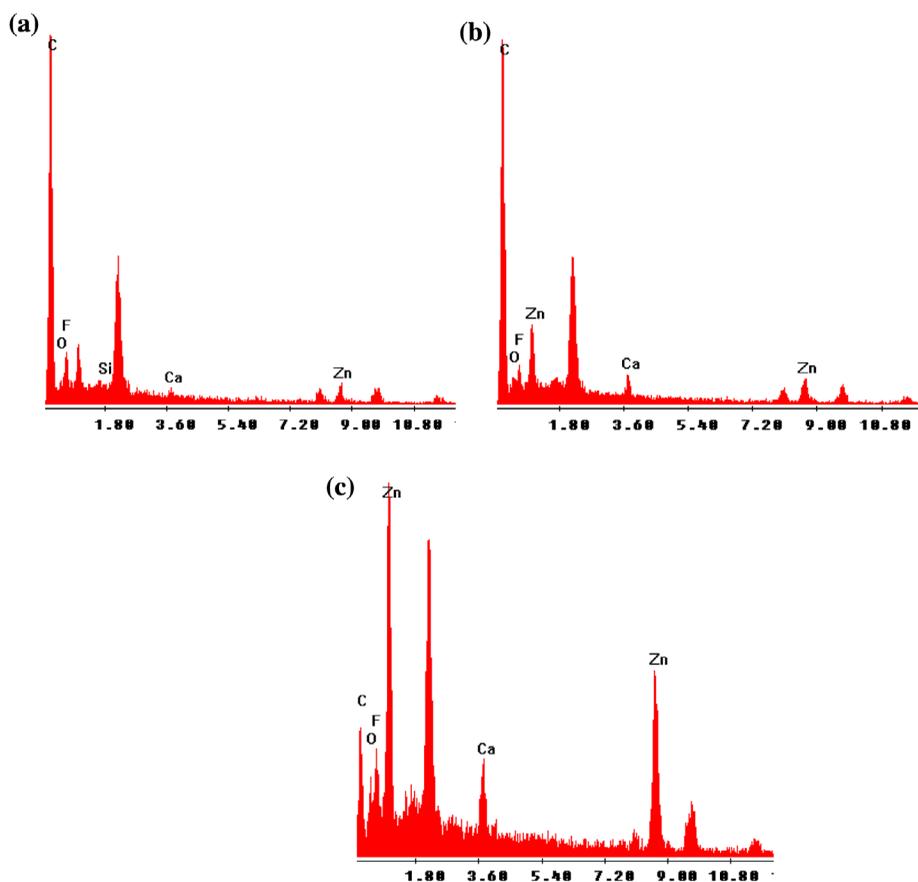
Figure 3. The EDX spectra of (a) CNT/FE-560 ºC, (b) CB/FE-560 ºC and (c) FE-560ºC.

composition of the residue in heating–cooling TGA runs for all compounds under study which were extracted from EDX results (Figures 3 and 4).

From Figure 2, at low temperatures, after cooling scan of CNT/FE-560 °C sample, 19.0% of nanocomposite remained. If this amount is multiplied by weight% of each element in Table 4, the weight% of that element based on the initial nanocomposite can be obtained.
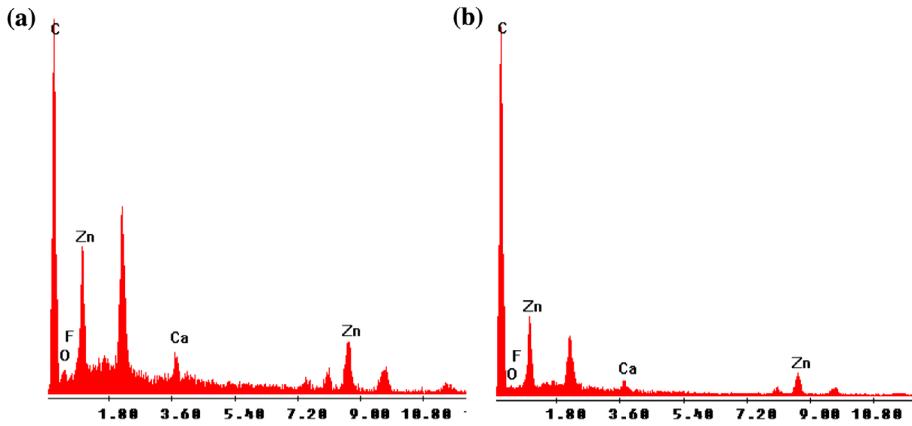
Figure 4. The EDX spectra of (a) CNT/FE-900 ᵒC and (b) CB/FE-900 ᵒC.

Table 5. Amount of element remained based on initial weight of compound.

Element	Element remained (%)				
	FE-560 °C	CB/FE-560 °C	CNT/FE-560 °C	CB/FE-900 °C	CNT/FE-900 °C
C	3.4	10.9	13.1	5.9	6.3
F	0.9	1.5	2.0	0.2	0.2
Zn	2.1	2.1	1.8	1.1	2.0
Ca	0.3	0.3	0.2	0.1	0.2
Si	–	–	0.1	–	–

The same procedure was done for all specimens. Results of these calculations are presented in Table 5.

These results show that the percentage of carbon and fluorine in the residue of TGA scan of CNT/FE-560 °C are more compared to the CB/FE-560 °C. The amount of residue in each of these samples is higher than that of FE-560 °C. This proves that CNT is able to preserve more FE from degradation compared to the samples containing CB or unfilled FE. In this aspect, indeed the CB-filled samples also act better than unfilled FE. Similarly, based on EDX results and considering work of Pham et al. [6] as mentioned earlier, it can be seen that FE attached or near the CNT at higher temperature range exhibit lower degradation tendency. Considering this and the fact that more carbon and fluorine remained in this nanocomposite residue after TGA run, it can also be concluded that more amount of FE remained undegraded or less degraded especially near CNT. The amount of remaining fluorine represents the undegraded FE. Therefore, it can be predicted that if more CNT is used in the initial FE, more FE can be saved in the undegraded or less degraded form in TGA scans up to 560 °C and most probably a highly CNT-filled FE will not be degraded up to this temperature.

3.1.3. EDX analysis – undegraded FE and char

At 560 °C, the 'undegraded FE + char' for CNT/FE-560 °C can also be calculated, by subtracting the percentage of 'CNT remained' in the nanocomposite (Table 2) from the percentage of 'C + F' in EDX analysis at 560 °C. Thus, the percentage of 'undegraded FE + char'

for CNT/FE-560 °C is 7.0% and for CB/FE-560 °C is 4.0%, again showing more percentage of 'undegraded FE + char' in the case of using CNT as filler for FE.

The increased decomposition temperatures caused using CNT in FE [6] are due to several reasons. Firstly, the presence of CNT in FE makes the active centers of FE main chains inactive, preventing the degradation, therefore can save FE nearer to the CNT surface. Secondly, the interactions between CNT and FE results in increased physical and chemical cross-linking points which prevent the degradation of the polymer chains. Besides, considering that the degradation of FE is a radical chain reaction, it is therefore susceptible to inhibition by reagents capable of trapping such radicals. Furthermore, the antioxidant nature of CNT attributed to its high electron affinity (≈2.65 eV) enables it to act as a radical scavenger. Consequently, CNT helps to trap radicals and inhibiting degradation of FE nearer to it. Moreover, Endo et al. [3] reasoned that thermal stability of FE near CNT is due to the presence of bounded rubber to CNT and concluded that this structure can prevent the decomposition of rubber at high temperatures by resisting the molecular mobility.

Table 5 also shows that when CB/FE-900 °C and CNT/FE-900 °C, were run up to 900 °C, much less fluorine and carbon remained compared to CB/FE-560 °C and CNT/FE-560 °C. These results indicate that most of the undegraded FE at temperatures below 560 °C was degraded from 560 °C up to 900 °C in both CNT/FE and CB/FE. From the EDX results (Table 5), the remaining C in CB/FE-900 °C and CNT/FE-900 °C are the same (C% consist of 'char + CNT' in CNT/FE and 'char + CB' in CB/FE). Considering this factor and TGA results of CNT and CB (Figure 1), it can be inferred that at 900 °C, char% in CNT/FE-900 °C is higher compared to that in CB/FE-900 °C and CNT% in CNT/FE-900 °C is lower relative to CB% in CB/FE-900 °C (CB degraded less than CNT at 900 °C as seen in Figure 1). Therefore, the char in CNT/FE-900 °C is still higher than in CB/FE-900 °C at 900 °C. Considering this factor and the results in Table 5, it can be suggested that in CNT/FE, most of the char is stable up to 900 °C, while in CB/FE, most of the char decomposed and only CB and mineral fillers remained at this temperature.

Comparing Zn% in CNT/FE-560 °C and CNT/FE-900 °C (Table 5), it shows that the amount of Zn in CNT/FE is almost unchanged and did not undergo any reaction up to 900 °C. On the other hand, the Zn% in CB/FE-560 °C and CB/FE-900 °C shows that some amount disappeared up to 900 °C. This is due to the reaction of ZnO with carbon at high temperature, producing vaporized Zn. Such reaction of ZnO and C at high temperature was reported by Gokon et al. [21].

3.2. Effect of thermal aging on residual elemental composition

Figure 5 is a representative figures of EDX obtained for aged and unaged samples. The elemental weight percent extracted from these figures are presented in Table 6. This table shows the surface composition of the composites before and after aging. The major elements in the composites are C, O, F, and Si. The initial loss in element is defined as the percentage lost due to aging for the different periods of time. The percentage loss can be calculated as follows: For 100 g of unaged FE (Table 6), there were 34.3, 5.0, 59.8, and 0.9 g of C, O, F, and Si, respectively. After 72 h of aging, if C_{rem}, O_{rem}, and F_{rem} g of C, O, and F, respectively, remained and C_{los}, O_{los}, and F_{los} g of C, O, and F, respectively, were lost. Then;

$$C_{rem} + C_{los} = 34.3\,g \,; O_{rem} + O_{los} = 5.0\,g \,and\, F_{rem} + F_{los} = 59.8\,g \qquad (1)$$
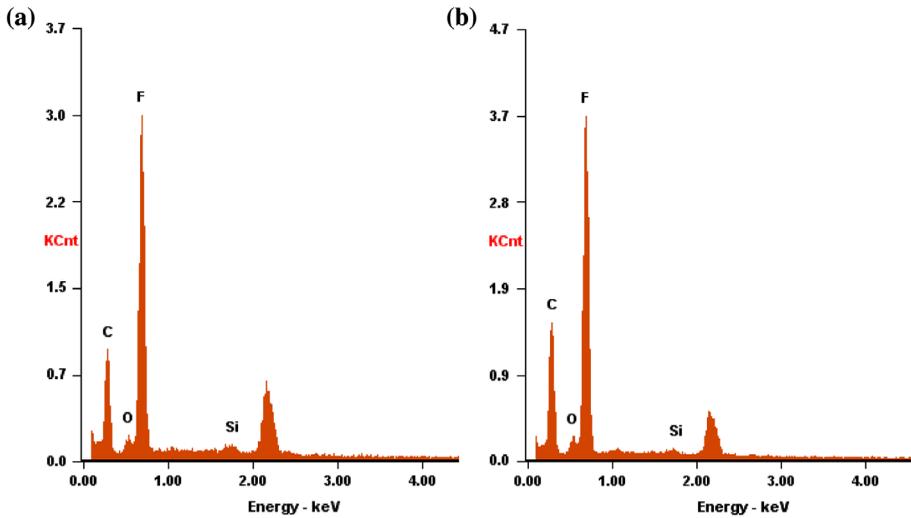
Figure 5. EDX spectra of (a) CNT/FE and (b) CNT/FE-72.

Table 6. The surface composition of the composites before and after aging, obtained by EDX.

	Wt%	At%	Wt%	At%	Wt%	At%	Wt%	At%
Element	FE		FE-24		FE-48		FE-72	
C	34.3	45.0	–	–	30.7	41.0	30.9	41.4
O	5.0	4.9	–	–	3.9	4.0	04.8	04.8
F	59.8	49.6	–	–	64.0	54.2	62.0	52.5
Si	0.9	0.5	–	–	1.4	0.8	2.3	1.3
Total	100	100	–	–	100	100	100	100
Element	CB/FE		CB/FE-24		CB/FE-48		CB/FE-72	
C	37.2	48.2	33.7	44.5	43.8	54.8	31.2	42.3
O	3.2	3.1	5.2	5.1	10.4	9.8	8.4	8.6
F	58.6	48.1	58.7	49.0	42.9	33.9	51.1	43.7
Si	1.0	0.6	2.4	01.4	2.9	1.5	9.3	5.4
Total	100	100	100	100	100	100	100	100
Element	CNT/FE		CNT/FE-24		CNT/FE-48		CNT/FE-72	
C	35.4	46.2	36.7	47.9	32.0	42.6	30.9	41.4
O	3.6	3.3	2.8	2.7	3.5	3.5	3.7	3.7
F	60.0	50.0	58.6	48.3	62.9	53.0	63.6	53.9
Si	1.0	0.5	1.9	1.1	1.6	0.9	1.8	1.0
Total	100	100	100	100	100	100	100	100

Since Si is not lost during aging, the amount of Si after 72 h of aging is 0.9 g. If T is the total weight of the remaining elements, then; $T = C_{rem} + O_{rem} + F_{rem} + 0.9\,g$

After 72 h of aging, the weight percentage of Si is 2.3% (Table 6), therefore; $\frac{0.9}{T} = 0.023$, and thus $T = 39.7\,g$. Using T and the percentage of C (Table 6), after 72 h of aging (30.9%), C_{rem} can be calculated as, $0.309 = \frac{C_{rem}}{T}$. Thus, $C_{rem} = 0.309 \times 39.7 = 12.3\,g$. $C_{los} = 34.3 - C_{rem} = 22.0\,g$.

Table 7. Initial element loss percentage after aging compared to unaged samples.

Element	Initial element loss%		
	FE-24	FE-48	FE-72
C	–	41.2	64.3
O	–	48.1	62.3
F	–	29.7	58.9
Si	–	0	0
Element	CB/FE-24	CB/FE-48	CB/FE-72
C	60.6	57.3	90.3
O	29.2	0	69.4
F	56.4	73.5	90.0
Si	0	0	0
Element	CNT/FE-24	CNT/FE-48	CNT/FE-72
C	46.7	43.3	52.0
O	60.2	38.4	43.6
F	49.9	34.1	41.6
Si	0	0	0
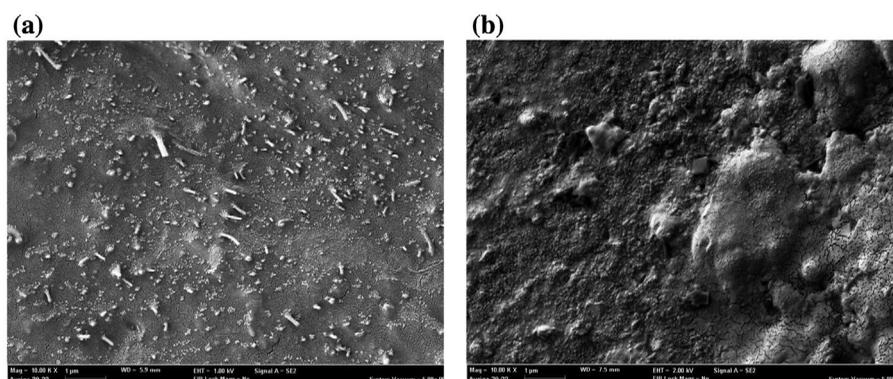
Figure 6. FESEM images of (a) CNT/FE (the razor-cut cross section surface) and (b) CNT/FE -72 (normal flat surface).
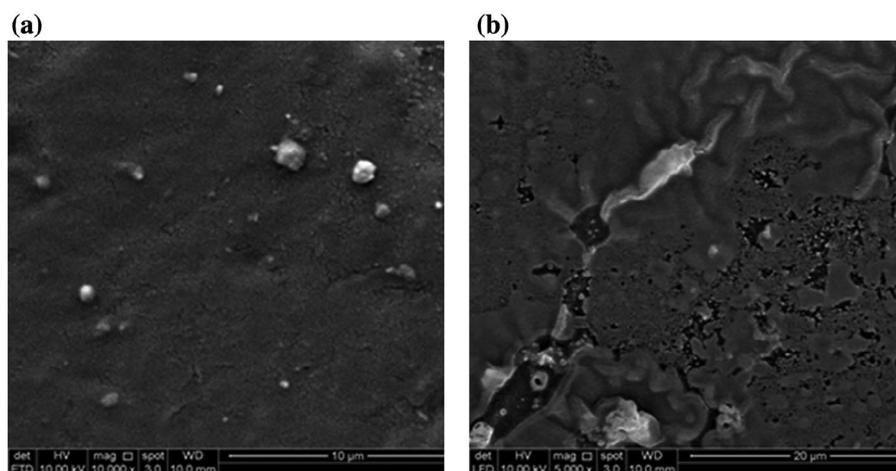
Figure 7. FESEM images of (a) FE and (b) FE-24.
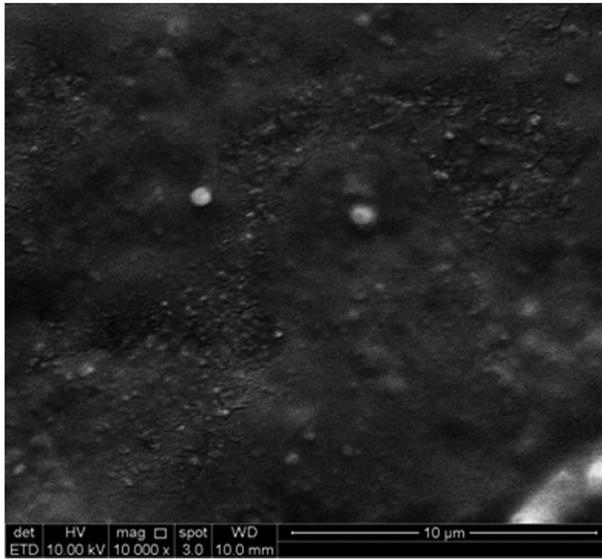
Figure 8. FESEM images of CB/FE -48.
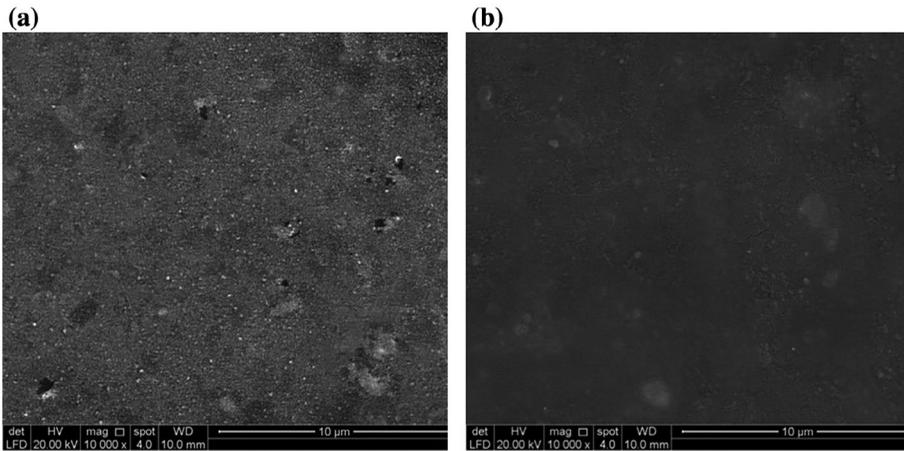
Figure 9. FESEM images of (a) CNT/FE and (b) CNT/FE-24.

Therefore, the percentage of C_{los} is,

$$C_{los}(\%) = \frac{\text{Wt. of } C_{los}}{\text{Wt. of initial C}} \times 100\,(\%) = \frac{22.1}{34.3} \times 100\,(\%) = 64.2\,\% \qquad (2)$$

This means 64.2% of the initial C is removed from the surface after 72 h of aging at 250 °C. The same calculations were done for F and O in all other aged composites. Results of these calculations are presented in Table 7. These results show that for each composite, with increasing aging time, the percentage loss of C, O, and F increases. This is because as the aging time increases, more degradation including dehydrofluorination, defluorination, and carbon–oxygen reactions occurred especially at the surface.[20] The results also show that
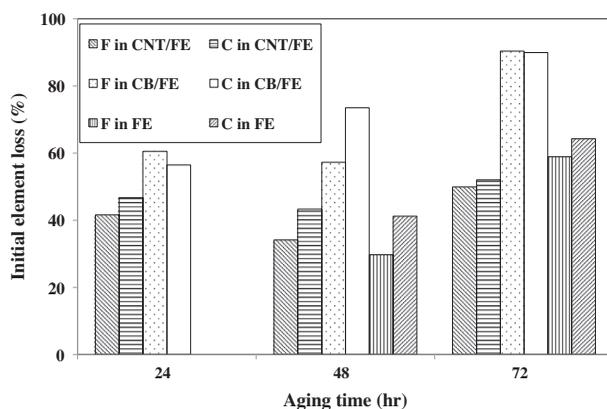
Figure 10. Initial element loss (%) at different aging times of FE and filler/FE.

at each aging time, the loss % of elements is in the following order: CNT/FE < FE < CB/FE. Therefore, CNT can preserve a larger portion of the elastomer surface from degradation. Comparing the results of FE and FE/CB, it also can be seen that for FE without CB, the loss of the elements are lower than in the one with CB. This could be due to the fluorination of CB,[20] leading to more loss of F and C.

The same reasons adduced for saving more percentage of undegraded FE and char in TGA runs are also valid for the thermal aging of CNT/FE. Besides, the antioxidant nature of CNT which is attributed to its high electron affinity (around 2.65 eV), enables it to act as radical scavenger [6] especially for oxide radicals produced due to the presence of air. This also helps to trap radicals, thereby inhibiting the degradation of nearby CNT, and resulting in increased percentage of undegraded FE.

A considerable depletion of F and C on the surface and to the depth of around 10–15 μm of cross section of CB/FE seals aged in oil containing amine-based dispersant at 150 °C also was reported by Smith et al. [20]. The authors reported that polytetrafluoroethylene (PTFE) also began to soften and released F at around 200–220 °C. This may explain the apparent susceptibility to heating in air shown by elastomer with a high TFE content.

A drastic decrease in C and F due to thermal aging in air at 200 °C from the surface of CB/FE (up to the depth of 5 nm) was also reported by Wang et al. [22]. As can be seen in Table 6, for CNT/FE, up to 24 h of aging, the initial percentage loss of each element increases. Nevertheless, as the aging time increases to 48 h, a decrease in percentage loss is observed. This is expected, due to the surface migration of fluoro groups; CF, CF_2, and CF_3. The same phenomenon was also reported by Wang et al. [22] for CB/FE.

Figure 6 shows the FESEM images of CNT/FE and CNT/FE-72 surfaces. As can be seen, due to aging, the amount of crack, as well as voids or masses appearing on the surface are slightly increased. Figures 7–9 show the FESEM images of FE and FE-24, CB/FE-48, CNT/FE, and CNT/FE-24, respectively. From these figures it can also be seen that after aging, the surface of FE and CB/FE seemed to undergo severe degradation with cracks, voids, and rougher surface. However, the surface of CNT/FE-24 is less affected. This also proves that CNT increases the thermal stability of aged specimens. Figure 10 shows the initial loss of element at different aging times for filler/FE, which was explained previously.

References

[1] PSP Global. Comparison of general use and high performance grades of Viton. Colorado: Technical Data Sheet; [cited 2015 Aug 19]. Available from: http://www.pspglobal.com/nfVitongrades.html.

[2] Fuller RE. Advanced polymer architecture sealing solutions for oil and gas applications. Seal. Tech. 2006;2006:6–11.

[3] Endo M, Noguchi T, Ito M, et al. Extreme-performance rubber nanocomposites for probing and excavating deep oil resources using multi-walled carbon nanotubes. Adv. Funct. Mater. 2008;18:3403–3409.

[4] He L, Xu Q, Hua C, et al. Effect of multi-walled carbon nanotubes on crystallization, thermal, and mechanical properties of poly(vinylidene fluoride). Polym. Compos. 2010;31:921–927.

[5] Chae DW, Hong SM. Rheology, crystallization behavior under shear, and resultant morphology of PVDF/multiwalled carbon nanotube composites. Macromol. Res. 2011;19:326–331.

[6] Pham TT, Sridhar V, Kim JK. Fluoroelastomer–MWNT nanocomposites-1: dispersion, morphology, physico-mechanical, and thermal properties. Polym. Compos. 2009;30:121–130.

[7] Russell T, Walder J, Rich A. The use of carbon nanotubes to improve conductive elastomers. Seal. Tech. 2005;2005:12–14.

[8] Levi N, Czerw R, Xing S, et al. Properties of polyvinylidene difluoride-carbon nanotube blends. Nano Lett. 2004;4:1267–1271.

[9] Ito M, Noguchi T, Ueki H, et al. Carbon nanotube enables quantum leap in oil recovery. Mater. Res. Bull. 2011;46:1480–4.

[10] He L, Sun J, Zheng X, et al. Effect of multiwalled carbon nanotubes on crystallization behavior of poly (vinylidene fluoride) in different solvents. J. Appl. Polym. Sci. 2011;119:1905–1913.

[11] Xu Y, Zheng W-T, Yu W-X, et al. Crystallization behavior and mechanical properties of poly (vinylidene fluoride)/multi-walled carbon nanotube nanocomposites. Chem. Res. Chin. Univ. 2010;26:491–495.

[12] Mago G, Fisher FT, Kalyon DM. Deformation-induced crystallization and associated morphology development of carbon nanotube-PVDF nanocomposites. J. Nanosci. Nanotechnol. 2009;9:3330–3340.

[13] Chen W, Li F, Han G, et al. Tribological behavior of carbon-nanotube-filled PTFE composites. Tribol. Lett. 2003;15:275–278.

[14] Sementsov YI, Gavrilyuk N, Prikhod'ko G, et al. Properties OF PTFE–MWNT composite materials. In: Schur DV, Zaginaichenko SY, Veziroglu TN, editors. Hydrogen materials science and chemistry of carbon nanomaterials: Springer; 2007. p. 757–763.

[15] Yu S, Zheng W, Yu W, et al. Formation mechanism of β-phase in PVDF/CNT composite prepared by the sonication method. Macromolecules. 2009;42:8870–8874.

[16] Mago G, Kalyon DM, Fisher FT. Membranes of polyvinylidene fluoride and PVDF nanocomposites with carbon nanotubes via immersion precipitation. J. Nanomater. 2008;2008:17:1–8.

[17] Huang S, Yee WA, Tjiu WC, et al. Electrospinning of polyvinylidene difluoride with carbon nanotubes: synergistic effects of extensional force and interfacial interaction on crystalline structures. Langmuir. 2008;24:13621–13626.

[18] Wen R, Ke K, Wang Y, et al. Interfacial interaction of polyvinylidene fluoride/multiwalled carbon nanotubes nanocomposites: a rheological study. J. Appl. Polym. Sci. 2011;121:3041–3046.

[19] Park E, Hong S, Park D, et al. Preparation of conductive PTFE nanocomposite containing multiwalled carbon nanotube via latex heterocoagulation approach. Colloid. Polym. Sci. 2010;288:47–53.

[20] Smith G, Park D, Titchener K, et al. Surface studies of oil-seal degradation. Appl. Surf. Sci. 1995;90:357–371.

[21] Gokon N, Hasegawa N, Kaneko H, et al. Photocatalytic effect of ZnO on carbon gasification with CO_2 for high temperature solar thermochemistry. Sol. Energ. Mater. Sol. C. 2003;80:335–341.

[22] Wang Y, Liu L, Luo Y, et al. Aging behavior and thermal degradation of fluoroelastomer reactive blends with poly-phenol hydroxy EPDM. Polym. Degrad. Stabil. 2009;94:443–449.

[23] Heidarian J, Hassan A. Microstructural and thermal properties of fluoroelastomer/carbon nanotube composites. Compos. Part B Eng. 2014;58:166–174.

[24] Heidarian J, Hassan A. Microstructural and thermal properties of fluoroelastomer/acidic surface modified carbon nanotube nanocomposites. Polym. Compos. Forthcoming 2015.

[25] Heidarian J, Hassan A, Normasmira AR. Improving the thermal properties of fluoroelastomer (Viton GF-600S) using acidic surface modified carbon nanotube. Polímeros. 2015;25:392–401.

[26] Heidarian J, Hassan A. Improving thermal properties of fluoroelastomer using carbon nanotubes in presence of air and under nitrogen flow. Asian J. Chem. 2015;27:1235–1239.